SYSTEMATIC STUDIES OF THE MICROBUNCHING AND WEAK INSTABILITY AT SHORT BUNCH LENGTHS

M. Brosi*, E. Blomley, T. Boltz, E. Bründermann, M. Caselle, J. Gethmann, B. Kehrer, A. Papash, L. Rota†, P. Schönfeldt‡, P. Schreiber, M. Schuh, M. Schwarz, J. L. Steinmann§, M. Weber and A.-S. Müller, Karlsruhe Institute of Technology, Karlsruhe, Germany
P. Kuske, Helmholtz Zentrum Berlin, Berlin, Germany

Abstract

At KARA, the Karlsruhe Research Accelerator of the Karlsruhe Institute of Technology synchrotron, the so-called short-bunch operation mode allows the reduction of the bunch length down to a few picoseconds. The microbunching instability resulting from the high degree of longitudinal compression leads to fluctuations in the emitted terahertz radiation. For highly compressed bunches at KARA, the instability occurs not only in one but in two different bunch-current ranges that are separated by a stable region. The additional region of instability is referred to as short-bunch-length bursting or weak instability. We will presents measurements of the threshold currents and fluctuation frequencies in both regimes. Good agreement is found between the measurement and numerical solutions of the Vlasov-Fokker-Planck equation. This contribution is based on the PRAB paper Phys. Rev. Accel. Beams 22, 020701 [1].

MOTIVATION

In the short-bunch operation mode of KARA the bunch length is reduced down to a few picoseconds. Due to this, coherent synchrotron radiation (CSR) in the sub-THz frequency range is emitted by the electron bunches. This coherent synchrotron radiation can act back on the electrons of the bunch as additional potential. This leads to a position dependent energy gain. As the electrons have slightly different paths around the ring depending on the magnet optics, this change in the energy distribution results in substructures in the longitudinal charge density. Under certain conditions the micro-bunching instability occurs as these substructures lead to the emission of CSR at higher frequencies causing a self-amplification. The wake potential growing stronger causes intense bursts of CSR emission in the THz frequency range. Such a burst is shown in Fig. 1. The name giving micro-structures on the charge distribution in the longitudinal phase space are displayed for three points in time during the burst in emitted CSR.

As shown in simulations (e.g. [2]) and by measurements at several electron storage rings (e.g. [3–6]), the micro-bunching instability occurs above a certain threshold current, which depends on different parameters, like the momentum compaction factor or the bunch length.

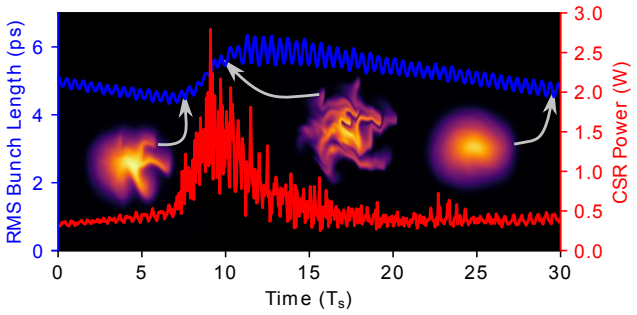

Figure 1: Simulation showing a burst in emitted CSR power (red) as well as the corresponding bunch length (blue) as a function of time (given in synchrotron oscillation periods T_s). For three time steps, the charge distribution in the longitudinal phase space is displayed, showing the corresponding structures. The simulation was performed with the Vlasov-Fokker-Planck solver Inovesa [7, 8].

The instability can be diagnosed and observed by detecting the changes in the CSR power emitted by each bunch over its revolutions. This is achieved at KARA with fast THz detectors and the readout system KAPTURE, as described in the next section (see also [4]). Multiple aspects (e.g. the threshold current) of the instability have already been studied and described in detail in e.g. [1, 3, 4, 9–13].

One aspect studied in detail is the behavior of the micro-bunching instability at low bunch currents and small rms bunch length of approximately two picoseconds and less. Under these conditions an additional region of instability occurs below the previously mentioned threshold current, which is referred to as short-bunch-length bursting. In the following, an overview is given of the results concerning this second region of instability. First, a short description of the simple scaling law predicting the threshold currents based on simulations is given. Then the measurement setup and technique are introduced. At the end the experimental observations are described and compared to dedicated simulations.

PREDICTION OF THRESHOLD CURRENT

In [2] Bane, Cai and Stupakov introduced a simple, linear scaling law which describes the threshold current of the micro-bunching instability in dependence of the parameters of the electron beam. The scaling law was derived from simulations conducted with a Vlasov-Fokker-Planck solver.

* miriam.brosi@kit.edu
† now at SLAC, Stanford, USA
‡ now at DLR-VE, Oldenburg, Germany
§ on leave at Argonne National Laboratory, Lemont, IL, USA

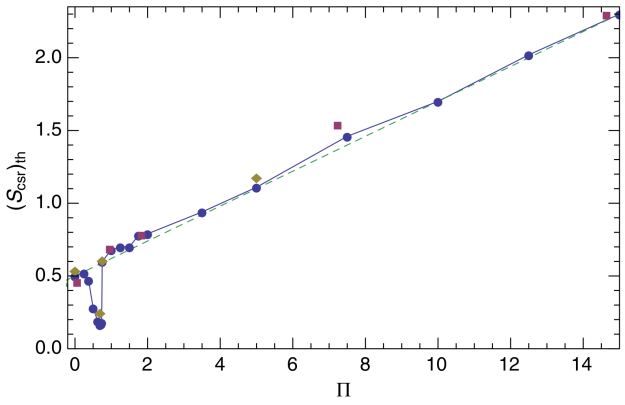

Figure 2: Simulated instability thresholds on which the simple linear scaling law was based, by [2]. "*For the CSR wake, threshold value of S_{csr} vs shielding parameter, $\Pi = \rho^{1/2}\sigma_{z0}/h^{3/2}$. Symbols give results of the VFP solver (blue circles), the LV code (red squares), and the VFP solver with twice stronger radiation damping (olive diamonds).*" ([2], figure 3).

The CSR impedance was considered in form of the parallel plates model, which simplifies the situation to a single electron bunch moving in vacuum on a circular trajectory between two perfectly conducting, infinitely large, parallel plates with the distance h equal to half of the height of the vacuum chamber.

The threshold current of the instability was given as [2]:

$$(S_{CSR})_{th} = 0.5 + 0.12\ \Pi \qquad (1)$$

Two dimensionless parameters Π and S_{CSR} were introduced as the shielding parameter $\Pi = \frac{\sigma_{z,0}\rho^{1/2}}{h^{3/2}}$ and the CSR strength $S_{CSR} = \frac{I_n\rho^{1/3}}{\sigma_{z,0}^{4/3}}$, with the normalized current $I_n = \frac{\sigma_{z,0}I_b}{\alpha_c\gamma\sigma_\delta^2 I_A}$. α_c is the momentum compaction factor, $\sigma_{z,0}$ the natural bunch length, ρ the bending radius, h half of the gap between the parallel plates, I_b the bunch current, $\sigma_{\delta,0}$ the natural energy spread, γ the Lorentz factor and I_A the Alfvén current[1].

Equation 1 was established by a linear fit to simulated threshold currents at different parameters (see Fig. 2). Low values of the shielding parameter Π correspond to short bunch length for fixed values of the vacuum chamber height $2h$ and the bending radius ρ. The "dip" visible in the simulated threshold currents around $\Pi \approx 0.7$ is caused by the short-bunch-length bursting. This additional region of instability was not considered in the linear scaling law (which is displayed as dashed line). The simulations further indicate that the extend to which this additional instability occurs not only depends on the value of the shielding parameter Π but also on the ratio of the longitudinal damping time to the period of the synchrotron frequency, given in from of the parameter $\beta = 1/(2\pi f_s \tau_d)$ [2]. This is also supported by the measurements discussed in [1, 13]. The instability is therefore often referred to as "weak instability".

[1] Alfvén current $I_A = 4\pi\varepsilon_0 m_e c^3/e = 17\,045$ A.

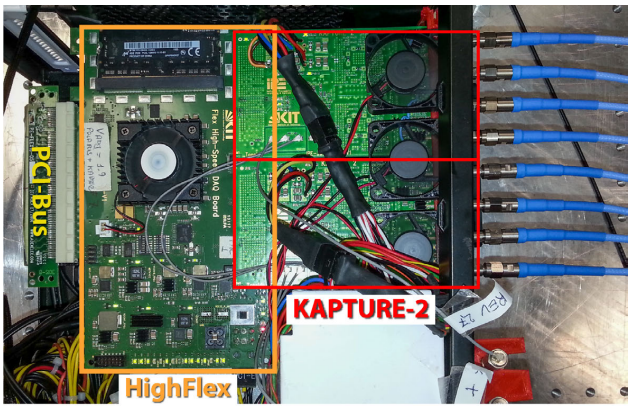

Figure 3: Photo of the KAPTURE-2 system consisting of two KAPTURE boards, the high-flex board with the FPGA and the PCI Bus connecting KAPTURE with the control PC [15]. Courtesy of Matthias Martin.

Further simulations were conducted at the exact parameters of the measurements (including same values of Π and β) to allow a detailed comparison [1].

MEASUREMENT SETUP AND METHOD

Fast THz detectors can be used to detect the changes in the emitted CSR power and gain insight into the dynamics under the influence of the micro-bunching instability. Room-temperature, zero-biased Schottky barrier diode detectors are commercially available with response times fast enough to resolve each bunch in a multi-bunch filling (RF frequency at KARA is 500 MHz). For the measurements presented in this contribution a quasi-optical, broad-band Schottky barrier diode detector from ACST GmbH [14], with a sensitivity range from 50 GHz to 2 THz and an analog bandwidth of 4 GHz (Pulse FWHM ≈130 ps), limited by an internal amplifier, was used.

As data acquisition system the in-house developed KAPTURE system was used. KAPTURE [16, 17] allows the simultaneous monitoring of all 184 possible bunches in KARA. KAPTURE consists of four sampling channels with a 12-bit ADC each. The idea behind KAPTURE was to selectively sample only the short detector pulses with four points and not the long "dark" time inbetween to save memory space and accomplish continuous sampling. The continuous turn-by-turn readout of the detector pulse for each bunch with 500 MHz results nevertheless in a data rate of 32 Gb/s. The newest version, KAPTURE-2 [18], provides eight sampling channels with up to 1 GHz sampling rate (Fig. 3).

A fast measurement method to gain information about the bunch-current dependent behavior of the instability could be established due to KAPTURE bunch-by-bunch capabilities [4]. The snapshot measurement method reduces the measurement time necessary for revealing the current dependence from hours to one second. As described in detail in [4, 13], the observed fluctuations in the emitted CSR power of each of the stored bunches in a multi-bunch filling pattern

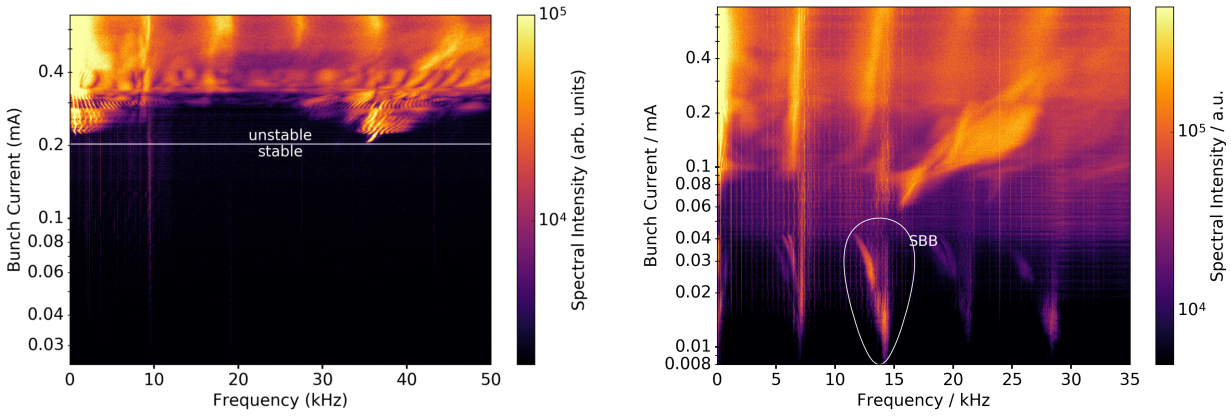

(a) (b)

Figure 4: Spectrograms of the fluctuations of the THz intensity as a function of the decaying bunch current, showing the micro-bunching instability. It was obtained in a single-bunch measurement lasting several hours while the bunch current decreased. In (a) no short-bunch-length bursting occurs, as the bunch was not compressed strongly enough. The natural bunch length was $\sigma_{z,0} = 3.8\,\mathrm{ps}$. (b) In this measurement the natural bunch length was reduced to $\sigma_{z,0} = 2.4\,\mathrm{ps}$ and the additional region of instability due to SBB is visible [1].

is used instead of just the information from a single bunch. The two spectrograms displayed in Fig. 4 are the result of a slow measurement of a single bunch while Fig. 5a show the result of a snapshot measurement focused on the bunch current region of interest.

A common way to visualize the dynamics of the instability is to display the fluctuation spectrum of the emitted CSR power, measured as a function of revolutions. These frequencies are directly connected to the frequencies of the dynamic processes changing the charge distribution in the longitudinal phase space. The current-dependency of these fluctuation frequencies is displayed in form of a spectrogram as shown in Fig. 4. The threshold current and other features of interest can be easily extracted in this representation.

OBSERVED SHORT-BUNCH-LENGTH BURSTING

As stated above, the second region of instability occurs only for highly longitudinally compressed bunches and is therefore referred to as short-bunch-length bursting (SBB). The measurements of the emitted CSR power are displayed as spectrograms to show the current-dependence of the fluctuation frequencies and to provide information about the dynamics of the instability. In Fig. 4a such a spectrogram is displayed for settings resulting in a natural bunch length of $\sigma_{z,0} = 3.8\,\mathrm{ps}$. The spectrogram shows the presence of fluctuations with different frequencies depending on the bunch current. Below the threshold current of about 0.2 mA no fluctuations due to the instability are present anymore. Figure 4b shows a measurement at settings where the SBB occurred ($\sigma_{z,0} = 2.4\,\mathrm{ps}$). Below the threshold current an additional region with fluctuations is visible. The fluctuation frequencies are also dependent on the bunch current and are located directly below twice and four times the synchrotron frequency.

RESULTS

Figure 5 shows a comparison of a snapshot measurement of the lower bunch current region showing the occurrence of the short-bunch-length bursting and the result of a simulation run for the same beam parameters. Both spectrograms show the additional region of instability due to the SBB below the main threshold current. While the bunch current values of the main threshold and the upper bound of the SBB coincide quite well, the current values of the lower bound differ slightly. The fluctuation frequencies in the emitted CSR power during the SBB are located directly below twice and four times the synchrotron frequency, which in the shown measurement is around $f_s = 6.55\,\mathrm{kHz}$. Also, the change observed in the fluctuation frequencies with decreasing bunch current is the same for the measurement and the simulation. The frequencies approach the 2nd (4th) harmonic of synchrotron frequency with decreasing current.

A scan over different values of Π (corresponding to different natural bunch lengths) was performed. The measured thresholds obtained during this scan will in the following be compared with Vlasov-Fokker-Planck solver simulations conducted individually for the beam parameters of each measurement. From each measurement and the corresponding simulation the main threshold current and, if present, the upper as well as lower bound of the short-bunch-length bursting was extracted. The values are displayed in Fig. 6 as a function of the shielding parameter Π. The simple linear scaling law for the main threshold current is shown as a grey, straight line.

Qualitatively, the simulated and measured thresholds show the same behavior. They both show the “dip” at approxi-

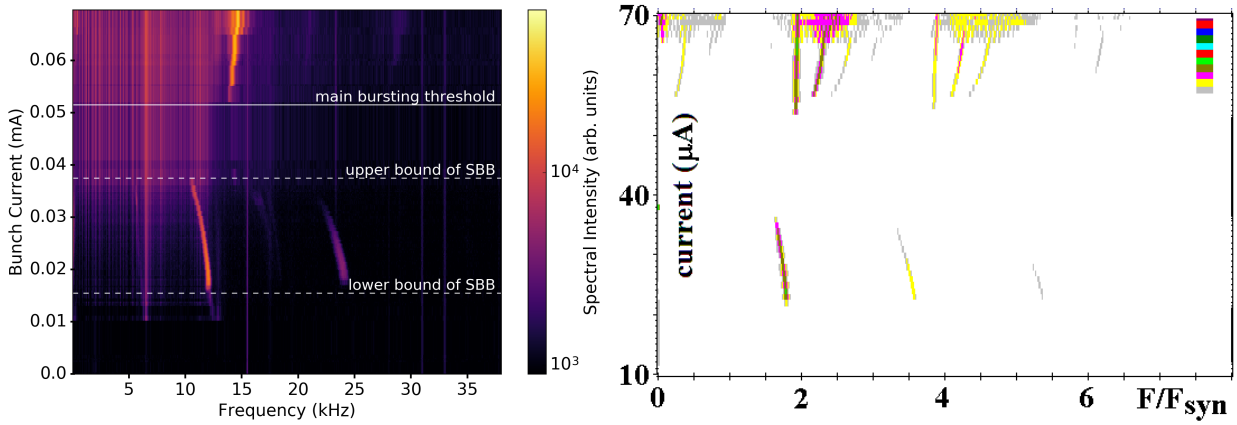

(a) (b)

Figure 5: Comparison of (a) a snapshot spectrogram of the fluctuations frequencies in the emitted CSR power as a function of bunch current. Below the end of the micro-bunching instability (main bursting threshold) around 0.052 mA, a second region of instability occurs between 0.038 mA and 0.016 mA. (b) Simulated spectrogram showing the end of the micro-bunching instability (main bursting threshold) around 0.054 mA as well as the short-bunch-length bursting between 0.036 mA and 0.022 mA. The frequencies of the SBB are in both spectrograms directly below two and four times the synchrotron frequency (f_s = 6.55 kHz). (Adapted from [1]).

mately $\Pi = 0.7$ which was not considered in the simple scaling law. Quantitatively, small differences are visible. The threshold in the results of the VFP solver are in general slightly higher than in the measurements. Also the range in Π where the SBB occurs is slightly smaller in the simulation results. This means, the measurements indicate the presence of instability also at parameters (current and Π) where the simulations predict only stable behavior. This is not easily explained by detector effects. One possible explanation for the small deviation could be slight fluctuations in the machine settings (e.g. noise on quadrupole power supplies). The measured thresholds would correspond more to the floor (the lowest observed threshold) while simulated would give an average value for the threshold.

Another possible explanation for the differences are the simplifications done in the simulations. The CSR impedance was approximated using the parallel plates model. This rather simple model does not consider any resistive wall or geometric impedances. In [19], for example, it was shown that an additional geometric impedance for an aperture slightly reduces the threshold current of the micro-bunching instability. Also the additional impedance of edge radiation leads to a slightly lower threshold current. This was not considered in the simulations. Last but not least, a stronger CSR-interaction than expected from the simple circular orbit simulated could be caused by an interaction extending into the straights behind the dipole magnets.

SUMMARY

For certain conditions a second region of instability can be observed below the threshold current of the longitudinal micro-bunching instability. This instability occurs at KARA in the short-bunch operation mode for $\alpha_c \leq 2.64 \times 10^{-4}$ and a high RF voltage resulting in a natural bunch length of $\sigma_{z,0} \leq 0.723$ mm $\hat{=}$ 2.43 ps and is therefore referred to as short-bunch-length bursting (SBB). Due to its dependence on the damping time it is also called weak instability. The measurements agree qualitatively with the simulation by [2] and the corresponding simple scaling law (Eq. 1). In comparison with the detailed simulations for each measurement point small differences could be revealed. Considering small additional impedances e.g. contributions by apertures and/or CSR-interaction extending further into the straight sections, could reduce the observed differences.

ACKNOWLEDGEMENTS

This work has been supported by the German Federal Ministry of Education and Research (Grant No. 05K16VKA). MB, PS, and JLS acknowledge the support by the Helmholtz International Research School for Teratronics.

REFERENCES

[1] M. Brosi *et al.*, "Systematic studies of the microbunching instability at very low bunch charges", *Phys. Rev. Accel. Beams* 22 (2019), Feb, 020701. `http://dx.doi.org/10.1103/PhysRevAccelBeams.22.020701`.

[2] K. L. F. Bane, Y. Cai, and G. Stupakov, "Threshold studies of the microwave instability in electron storage rings", *Phys. Rev. ST Accel. Beams*, vol. 13, p. 104402, Oct. 2010. `doi:10.1103/PhysRevSTAB.13.104402`

[3] A.-S. Müller *et al.*, "Far Infrared Coherent Synchrotron Edge Radiation at ANKA", in *Proc. 21st Particle Accelerator Conf. (PAC'05)*, Knoxville, TN, USA, May 2005, paper RPAE038.

[4] M. Brosi *et al.*, "Fast mapping of terahertz bursting thresholds and characteristics at synchrotron light sources", *Phys. Rev.*

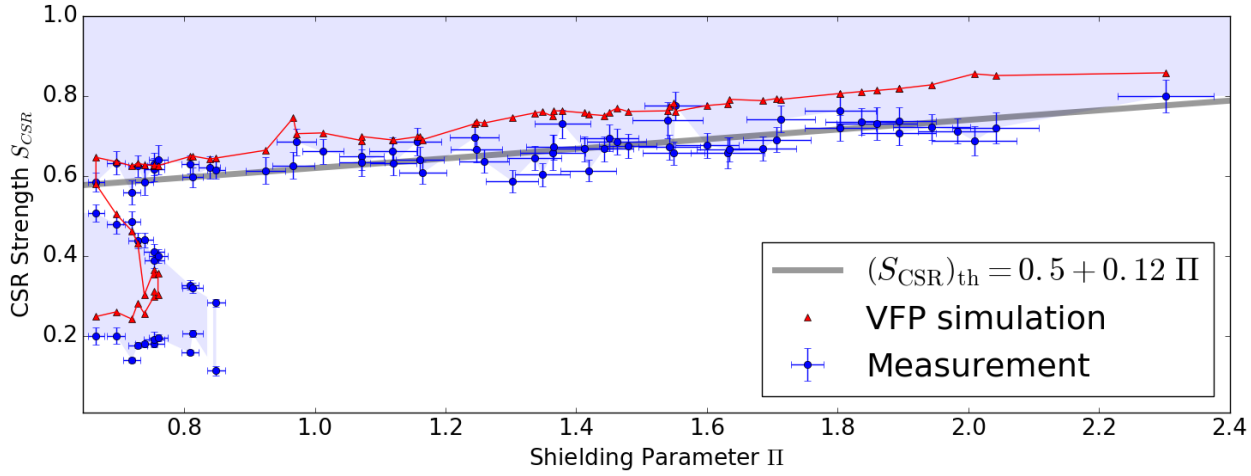

Figure 6: Threshold currents for different beam parameters gained from snapshot measurements and VFP solver simulations are displayed using the dimensionless parameters S_{CSR} and Π. The measured area of instability is indicated with a light blue shade and confined by the measured thresholds (blue discs) with the error bars displaying the standard deviation error of each measurement. The red triangles show the results of the VFP solver calculations at the corresponding beam parameters (red line to guide the eye). The linear scaling law for the main bursting threshold given by Eq. 1 is indicated by the gray line [1].

Accel. Beams, vol. 19, p. 110701, Nov. 2016. doi:10.1103/PhysRevAccelBeams.19.110701

[5] M. Ries *et al.*,"Thz bursting thresholds measured at the metrology light source," in Proceedings of 2012 International Particle Accelerator Conference (2012) p. 3030.

[6] W. Shields *et al.*,"Microbunch instability observations from a thz detector at diamond light source," Journal of Physics: Conference Series 357, 012037 (2012).

[7] P. Schönfeldt *et al.*, "Parallelized Vlasov-Fokker-Planck solver for desktop personal computers", *Phys. Rev. Accel. Beams*, vol. 20, p. 030704, Mar. 2017. doi:10.1103/PhysRevAccelBeams.20.030704

[8] P. Schönfeldt *et al.*, Inovesa/Inovesa: Gamma Two. (2018), Jul. http://dx.doi.org/10.5281/zenodo.1321580.

[9] M. Brosi *et al.*, "Studies of the Micro-Bunching Instability in Multi-Bunch Operation at the ANKA Storage Ring", in *Proc. 8th Int. Particle Accelerator Conf. (IPAC'17)*, Copenhagen, Denmark, May 2017, pp. 3645–3648. doi:10.18429/JACoW-IPAC2017-THOBA1

[10] M. Brosi *et al.*, "Studies of the Micro-Bunching Instability in the Presence of a Damping Wiggler", in *Proc. 9th Int. Particle Accelerator Conf. (IPAC'18)*, Vancouver, Canada, Apr.-May 2018, pp. 3273–3276. doi:10.18429/JACoW-IPAC2018-THPAK029

[11] M. Brosi *et al.*, "Synchronous Measurements of Electron Bunches Under the Influence of the Microbunching Instability", in *Proc. 10th Int. Particle Accelerator Conf. (IPAC'19)*, Melbourne, Australia, May 2019, pp. 3119–3122. doi:10.18429/JACoW-IPAC2019-WEPTS015

[12] J. L. Steinmann *et al.*, "Continuous bunch-by-bunch spectroscopic investigation of the microbunching instability", *Phys. Rev. Accel. Beams*, vol. 21, p. 110705, Nov. 2018. doi:10.1103/PhysRevAccelBeams.21.110705

[13] M. Brosi, "In-Depth Analysis of the Micro-Bunching Characteristics in Single and Multi-Bunch Operation at KARA", Ph.D. thesis, Karlsruhe Institute of Technology, 2020, defended, to be published.

[14] ACST GmbH, http://www.acst.de/

[15] M. Martin, "Rekonstruktion der Form von THz-Pulsen aus kurzen Elektronenpaketen mit hohen Wiederholraten an KARA", Master thesis, Karlsruhe Institute of Technology, 2019

[16] M. Caselle *et al.*, "An ultra-fast data acquisition system for coherent synchrotron radiation with terahertz detectors", *J. Instrum.*, vol. 9, p. C01024, Jan. 2014. doi:10.1088/1748-0221/9/01/C01024

[17] M. Caselle *et al.*, "Commissioning of an Ultra-fast Data Acquisition System for Coherent Synchrotron Radiation Detection", in *Proc. 5th Int. Particle Accelerator Conf. (IPAC'14)*, Dresden, Germany, Jun. 2014, pp. 3497–3499. doi:10.18429/JACoW-IPAC2014-THPME113

[18] M. Caselle *et al.*, "KAPTURE-2. A picosecond sampling system for individual THz pulses with high repetition rate", *J. Instrum.*, vol. 12, p. C01040, Jan. 2017. doi:10.1088/1748-0221/12/01/c01040.

[19] P. Schönfeldt, "Simulation and measurement of the dynamics of ultra-short electron bunch profiles for the generation of coherent THz radiation", Ph.D. thesis, Karlsruhe Institute of Technology, 2018, http://dx.doi.org/10.5445/IR/1000084466